

# Use of Ballast Support Condition Back-Calculator for Quantification of Ballast Pressure Distribution Under Concrete Sleepers

Z. Gao, M. S. Dersch, Y. Qian, M. V. Csenge, & J. R. Edwards  
*University of Illinois at Urbana-Champaign, Urbana, IL, USA*

**ABSTRACT:** In North America, most rail corridors are constructed using ballasted track. Monitoring the ballast support condition and improving upon current sub-structure/ballast maintenance strategies will ensure safe railroad operations. However, it is inherently difficult to evaluate the pressure distribution at the sleeper-ballast interface. Researchers at University of Illinois at Urbana-Champaign (UIUC) have developed an instrumentation strategy and analysis tool, the support condition back-calculator, to quantify ballast pressure distributions under concrete sleepers without interrupting the traffic. This laboratory-validated non-intrusive method uses concrete sleepers' bending moment profile and rail seat loads as inputs to back-calculate the reaction distribution through the use of an optimization algorithm. To better understand the in-service ballast support conditions, this technique was deployed in the field on a Class I heavy haul freight railroad in the United States. Concrete surface strain gauges were installed on concrete sleepers to measure their in-field bending moments. Wheel Impact Load Detectors (WILD) were used to measure rail seat input loads. The focus of this paper is to quantify the ballast pressure distributions beneath concrete sleepers on the heavy-haul tangent track. An evaluation of ballast pressure distribution variations between adjacent sleepers and through tonnage accumulation are also included. The information presented in this paper demonstrates the potential of the back-calculator for monitoring the ballast condition and will assist the rail industry in optimizing tamping cycle, enhancing safety, and developing more representative sleeper flexural designs for North America railroad applications.

## 1 INTRODUCTION AND BACKGROUND

Throughout the world, ballast is widely used for supporting railroad track infrastructure, and it is located between, below, and around the sleepers (Solomon 2001). However, due to ballast's granular property, repeated train loads can cause plastic deformation, which can eventually lead to ballast breakage, track settlement, and track geometry deviations (Selig & Waters 1994). To prevent these ballast deterioration mechanisms from jeopardizing safe railroad operations, advanced techniques have been employed in recent years to inspect and quantify the ballast condition, including using hi-rail-based ground penetrating radar (GPR) systems (Sussmann et al. 2003, Thompson & Carr 2014), and installing Matrix Based Tactile Surface Sensors (MBTSS) systems along the bottom of the sleepers (McHenry 2013). However, several issues exist within those techniques. For instance,

GPR inspections do not facilitate continuous monitoring of ballast condition under revenue service train passes, and the installation of MBTSS requires disturbing the ballast. Therefore, it is necessary to have a non-intrusive technique to accurately and continuously measure the ballast support condition, directly below the sleeper, in a timely manner. Researchers at University of Illinois at Urbana-Champaign (UIUC) have developed a ballast support condition back-calculator, an indirect measurement and analysis technique to quantify the ballast support condition beneath concrete sleepers using concrete sleeper flexural data recorded under revenue service traffic. The primary focus of this paper is to present the preliminary ballast support conditions on a North American Class I heavy-haul freight track using the ballast support condition back-calculator.

## 2 BALLAST SUPPORT CONDITION BACK-CALCULATOR BACKGROUND

The methodology of the back-calculator is to use the rail seat loads and the bending moments along the concrete sleeper to back-calculate the ballast support condition beneath the sleeper. Based on force equilibrium and the basic principles of statics, for a two-dimensional subject, only one combination of reaction forces (one support condition) can account for a certain moment profile under a set of applied loads. Therefore, if the concrete sleeper is simplified as a two-dimensional beam, then its ballast support condition can be back-calculated from the sleeper's bending moments and the corresponding rail seat loads. To quantify the sleeper bending moments in the field concrete surface strain gauges were used to measure the bending strains of the sleeper, which were converted into bending moments using the appropriate calibration factors (RailTEC 2013). Rail seat loads are indirectly computed from wheel loads provided by a nearby Wheel Impact Load Detector (WILD) site using the recommended equation given in American Railway Engineering and Maintenance-of-Way Association (AREMA) Manual for Railway Engineering (MRE) (2016).

### 2.1 Two-dimensional sleeper model

To further simplify and bound the problem, a two-dimensional sleeper model, shown in Figure 1, was developed. The model represented a 260 cm (102 in.) long concrete sleeper typically used in North American heavy haul freight railroad, and it was divided into six discrete bins of equal size, with the width of each bin being 43 cm (17 in.). Each bin carried a certain percentage of the total ballast reaction force, and the reaction force within each bin was assumed to be uniformly distributed. The reaction force distribution in Figure 1 demonstrates a scenario where the ballast support is uniform along the entire sleeper, but it is not intended to represent an actual result from the back-calculator. Concrete surface strain gauges were generally placed along the top chamfer of the sleeper, and they were taken into account in the two-dimensional model (Fig. 1). The rail seat loads were assumed to be uniformly distributed over each of the 15 cm (6 in.) rail seats. The two-dimensional sleeper model includes two boundary conditions for computation. First, based on force equilibrium, the total

ballast reaction force should equal the total rail seat loads, thus the sum of all six bins should be 100%. Second, the value of each bin should not be less than 0, as it is unrealistic to have a negative reaction force.

### 2.2 Optimization process

Once the two rail seat load magnitudes are input into the back-calculator, it then executes an optimization process to generate combinations of reaction forces that could satisfy the two boundary conditions. For each reaction force combination, the back-calculator would generate the bending moment profile of the sleeper based on the rail seat loads and compare it to the actual input bending moment profile. The optimization process stops when the difference between the calculated and actual bending moment profiles reached its minimum, and the reaction force combination that generated this calculated bending moment profile became the resultant support condition. The ballast reaction forces could then be converted into ballast pressures by dividing the forces over the bottom width of the sleeper. In the optimization process, Simulated Annealing and Bi-polar Pareto Distribution were used as the optimization algorithm and the random variable generator. The benefits of implementing them together were that they could find better solutions in less time (Englander & Englander 2014), and they were able to avoid getting stuck in local optima (Kirkpatrick et al. 1983). The maximum computational time for a given set of inputs was approximately one minute, which was considered to be short and reasonable for achieving the objectives associated with the back-calculator.

## 3 FIELD EXPERIMENTATION PLAN

To estimate and analyze the field ballast conditions under revenue service loads using the ballast support condition back-calculator, field experimentation was conducted at a tangent location on a Class I heavy haul freight railroad in the United States. The sleepers installed at this location had the same length as that of the two-dimensional sleeper model, and the concrete surface strain gauges were installed at the exact locations as those represented in the model to measure the bending moments experienced by the sleepers. As shown in Figure 2, the test site was divided into two zones, spaced approximately 18 m (60 ft) apart, with each zone consisting of five sleepers. Based on visual inspection, Zone 1 was selected as a poorly supported zone because, upon train passes, this zone was observed to deflect more than Zone 2 (Wolf 2015). Two thermocouples were installed on a sleeper between the two zones, one at the sleeper top chamfer and one near the sleeper bottom covered in

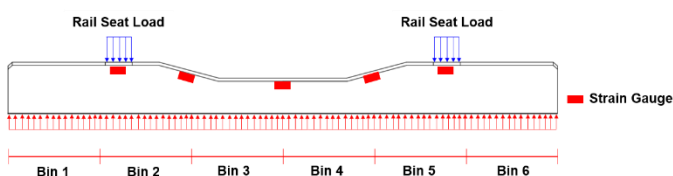


Figure 1. Two-dimensional sleeper model (with assumed uniform support condition).

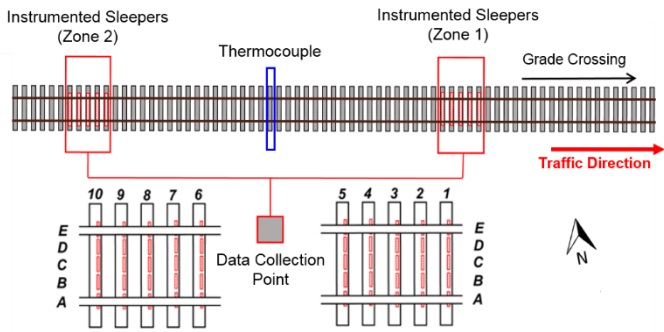


Figure 2. Class I mainline field experimentation site layout (Wolf et al. 2016).

ballast. These were deployed to measure the temperature gradient between top and bottom of the sleeper (Wolf et al. 2016). The wheel load data provided by the nearby WILD site were used to approximate the rail seat loads experienced by the sleepers. Since the wheels passing through the test site had a consistent nominal wheel load of 160 kN (36 kips), the rail seat load could be approximated to be 80 kN (18 kips) by using the AREMA recommended equation (AREMA 2016), and this value was used as the input rail seat loads for the support condition back-calculator.

#### 4 PRILIMINARY RESULTS FROM BALLAST SUPPORT CONDITION BACK-CALCULATOR

##### 4.1 Ballast pressure limit states

Ballast pressure distributions were used to present the resultant support conditions so that the back-calculator results could be correlated with AREMA recommended ballast properties. Three ballast pressure limit states were introduced to further aid the evaluation of the ballast condition.

1. The ballast pressure under an assumed uniform support condition was calculated to be 221 kPa (32 psi).
2. AREMA MRE specified the allowable ballast pressure under concrete sleepers to be 586 kPa (85 psi).
3. The ballast pressure corresponding to the AREMA allowable subgrade bearing stress of 172 kPa (25 psi) could be calculated using the Talbot equation below.

$$h = \left( \frac{16.8 p_a}{p_c} \right)^{4/5} \quad (1)$$

where,  $h$  = support ballast depth

$p_a$  = pressure at sleeper-ballast interface

$p_c$  = pressure at subballast-subgrade interface

Since the test site was considered to be well-maintained, the total depth of ballast and subballast was assumed to be 46 cm (18 in.) according to AREMA,

and the ballast pressure was then calculated to be 379 kPa (55 psi) from the equation above.

##### 4.2 Ballast pressure variations between sleepers

During a site visit on May 26<sup>th</sup>, 2015, flexural data were captured from a train pass at around 8 a.m. Figure 3 shows the resultant ballast pressure distribution when the instrumented sleepers were subjected to a single loaded axle from that train pass. The ballast pressure limit states can be seen in Figure 3 as three horizontal dashed lines. To better display the results, the uniformly distributed pressure within each bin was simplified into a single point located at the centerline of each bin and having the same magnitude as the uniform pressure. The points within six bins were connected together by straight lines to form the pressure distribution profile. To clearly depict the results in a single graph, only three out of five sleepers were selected from each zone.

Variation of ballast support conditions can be seen among adjacent sleepers. As shown in Figure 3, ballast pressures varied for all sleepers in both zones, but

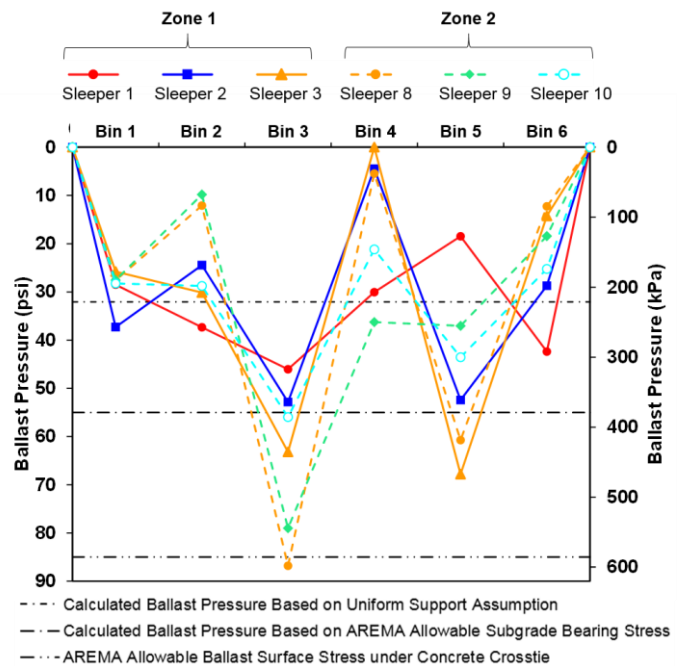


Figure 3. Ballast pressure distributions for six sleepers under one loaded axle from an 8 a.m. train on May 26<sup>th</sup>, 2015.

Zone 1 experienced a slightly higher variation, where the average percent difference among ballast pressure distributions in Zone 1 was 55%, 8% greater than the average percent difference in Zone 2. It is noticeable that the pressure in Bin 4 of Sleeper 3 was almost zero, which means that within Bin 4 of Sleeper 3, a void had developed at the sleeper-ballast interface. In addition, the ballast pressures of some sleepers exceeded the ballast pressure limit computed based on the allowable subgrade bearing stress. This indicates that subgrade bearing capacity failure could occur if this exceedance continued to happen. However, since the track was well-maintained, the actual ballast

pressure that would induce an excessive subgrade pressure could be higher than the current value, meaning that it is likely that this site would not experience a subgrade bearing capacity failure. The allowable ballast surface stress was also exceeded on a few occasions within Bin 3 of Sleeper 8. If this exceedance persisted, accelerated ballast deterioration could be expected.

### 4.3 Ballast Pressure Index

To better analyze the variation of ballast pressure beneath the sleepers, researchers at UIUC developed the Ballast Pressure Index (BPI), a quantifiable value that can evaluate the uniformity of ballast pressure distribution. BPI is simply defined as the ballast pressure computed from the back-calculator, normalized to the theoretical, uniform ballast pressure within each bin of the sleeper model (see equation below).

$$BPI = \frac{P_{comp}}{P_{uni}} \quad (2)$$

where, BPI = Ballast Pressure Index

$P_{comp}$  = pressure computed from the back-calculator

$P_{uni}$  = pressure based on the assumed uniform support

For a certain sleeper bin, if the ballast support satisfies the uniform support assumption, then the computed ballast pressure will be the same as the uniform ballast pressure, making the BPI equal 1. When a void develops in a sleeper bin, the computed ballast pressure becomes 0, so does the BPI for that particular bin. A sleeper bin is considered to be a hotspot if the computed ballast pressure exceeds the AREMA allowable ballast surface stress, because the exceedance indicates a high possibility of accelerated ballast deterioration, which poses a threat to the safe railroad operation. Therefore, for this particular test site, the BPI value of a hotspot is calculated to be 2.66 (586 kPa divided by 221 kPa).

Figure 4 shows the color-coded BPI distribution for all ten instrumented sleepers under the same loaded axle used in Figure 3. Green represents the uniform support scenario, where the BPI value is 1; blue represents voids, where the BPI value is 0; red represents hotspots, where the BPI value is no less than 2.66. The more consistent green there is for a sleeper shown in Figure 4, the more uniform the ballast support was beneath that sleeper. Following this logic, among all ten instrumented sleepers, Sleeper 1 and 10 had the most uniform support conditions. Besides demonstrating the uniformity of the ballast support condition, this color-coded BPI distribution can also pinpoint the voids and hotspots within the system. As can be seen in Figure 4, hotspots were solely developed within Zone 2, and next to each hotspot bin were

two adjacent bins showing bluish colors, suggesting that voids might develop somewhere within those bins. This significant BPI difference among the adjacent bins implies that those sleepers in Zone 2 were not as properly supported as those in Zone 1. The evaluation contradicts the visual inspection conducted at the beginning of the field installation, which considered Zone 1 as poorly supported. The contradiction not only indicates that visual inspection could be misleading sometimes, but also further justify the necessity to analyze the ballast support condition at the sleeper-ballast interface.

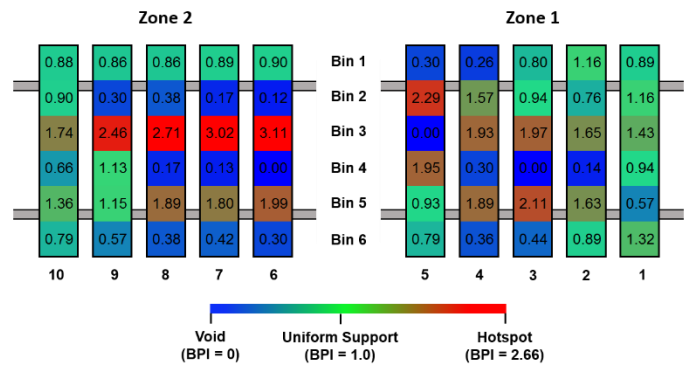


Figure 4. BPI distribution for ten sleepers under one loaded axle from an 8 a.m. train on May 26<sup>th</sup>, 2015.

### 4.4 Ballast pressure variations between months

In order to investigate the variation of ballast support conditions as a function of time or tonnage accumulation, two more site visits were made on July 8<sup>th</sup> and August 14<sup>th</sup>, 2015, and data were collected for a train pass at around 8 a.m. during both site visits. Figure 5 shows the BPI distributions from all three site visits. Similar to Figure 4, for each date, the BPI distribution was based on a single loaded axle of the 8 a.m. train. To clearly demonstrate all three BPI distributions on a single figure, each sleeper bin was cut into three sections from the bottom-left corner, with the left section representing the BPI value from May 26<sup>th</sup>, 2015, the middle section the BPI value from July 8<sup>th</sup>, and the right section the BPI value from August 14<sup>th</sup>. By doing so, the change in BPI value can be observed clockwise within each sleeper bin.

As illustrated in Figure 5, throughout the 4-month period and approximately 31.8 million gross tonnes (mgt) (35 million gross tons (MGT)) of tonnage accumulation, the BPI distribution for all ten sleepers stayed generally constant, as hotspots remained as hotspots and voids remained as voids. Among three site visits, the maximum BPI increase was 0.74 (or 163 kPa (23.6 psi) in ballast pressure), whereas the

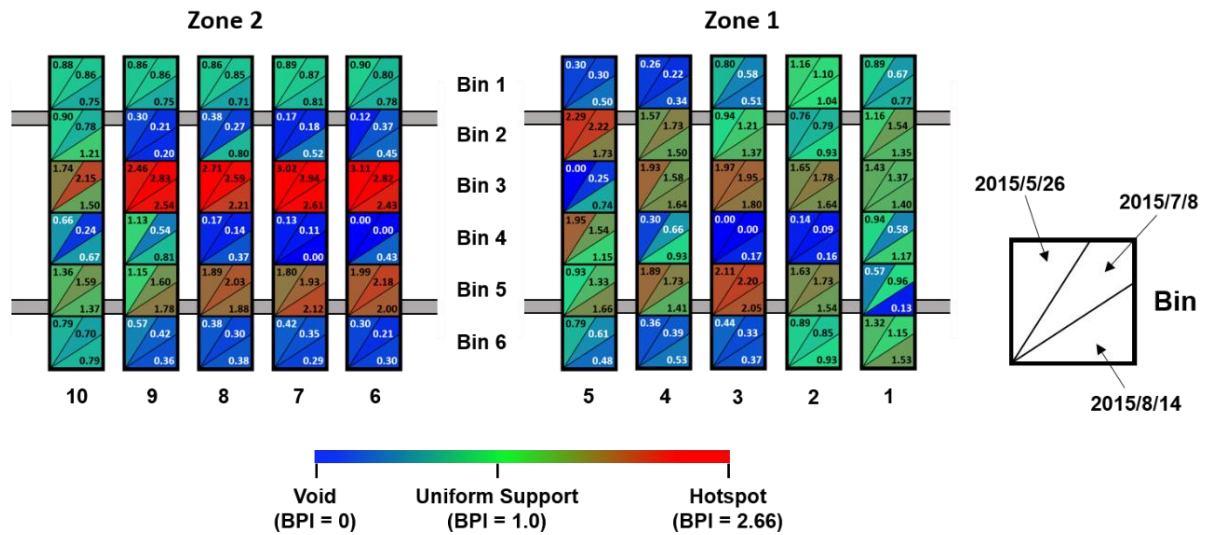


Figure 5. BPI distributions for three site visits on May 26<sup>th</sup>, July 8<sup>th</sup>, and August 14<sup>th</sup>, 2015.

maximum BPI decrease was 0.80 (or 176 kPa (25.6 psi) in ballast pressure).

One would expect that as tonnage increased, the ballast support condition would become more center-bound. However, this change in ballast support condition could not be easily observed in the test site. On the contrary, based on the BPI distributions, Zone 2 showed an exact opposite ballast behavior. Hotspots were predominant in Sleeper 6, 7, and 8 during the first site visit, but after four months, the BPI values for those hotspots decreased by 18% on average, and they were no longer above the hotspot limit of 2.66 (Fig. 5). Factors other than tonnage accumulation might have more impact on this change of ballast support condition, such as change in ballast moisture content, change in ballast particle shape, and change in temperature.

## 5 CONCLUSIONS

The ballast support condition back-calculator was developed as a tool to quantify the ballast condition at the sleeper-ballast interface. By using measured bending moments from concrete surface strain gauges installed at discrete locations along the sleeper and approximated rail seat loads calculated by wheel loads provided by WILD site, this non-intrusive analytical technique was implemented to back-calculate the in-service ballast support condition beneath concrete sleepers on a North American Class I heavy haul freight railroad. Several conclusions can be drawn from the preliminary results generated by the back-calculator for the field test site.

- Ballast pressure varied within each instrumented sleeper, as well as among adjacent sleepers.
- At times, the AREMA allowable subgrade bearing stress and ballast surface stress were exceeded. If this exceedance persisted

throughout a certain time or tonnage accumulation, accelerated ballast deterioration may occur.

- Color-coded BPI distribution provided an effective method to not only evaluate the uniformity of ballast distribution, but also identify the voids and hotspots at the sleeper-ballast interface.
- Based on data from three site visits, tonnage accumulation didn't seem to have a significant impact on the ballast pressure distribution, partially because the test site had been well-maintained.

## 6 ACKNOWLEDGEMENTS

Portions of this research effort were funded by U.S. National University Rail Center (NURail Center). The authors are grateful for the guidance and valuable feedback provided by Henry Wolf and Prof. Ouyang Yanfeng from UIUC during the development of the back-calculator. The authors would also like to thank Phanuwat Kaewpanya, and Quinn Todzo for their assistance with field experimentation and data processing. J. Riley Edwards has been supported in part by grants to the UIUC Railroad Engineering Program from CN, Hanson Professional Services, and the George Krambles Transportation Scholarship Fund.

## REFERENCES

- American Railway Engineering and Maintenance-of-Way Association (AREMA). 2016. *Manual for Railway Engineering (MRE)*. Lancaster, Maryland, USA.
- Englander, J.A. & Englander, A.C. 2014. Tuning Monotonic Basin Hopping: Improving the Efficiency of Stochastic Search as Applied to Low-Thrust Trajectory. In *Proceedings of International Symposium on Space Flight Dynamics 2014, May 2014*. Laurel, Maryland, USA.

- Kirkpatrick, S., Gelatt, C.D., & Vecchi M.P. 1983. Optimization by Simulated Annealing. *Science*, New Series, Vol. 220, No. 4598, pp. 671-680.
- McHenry, M.T. 2013. *Pressure Measurement at the Ballast-tie Interface of Railroad Track Using Matrix Based Tactile Surface Sensors*. M.S. Thesis 2013. University of Kentucky, Lexington, Kentucky, USA.
- RailTEC. 2013. FRA Improved Concrete Crossties and Fastening Systems for US High Speed Passenger Rail and Joint Passenger/Freight Corridors. Final Report. Railroad Transportation and Engineering CENTER (RailTEC), University of Illinois at Urbana-Champaign (UIUC), Urbana, Illinois. United States Department of Transportation (USDOT) Federal Railroad Administration (FRA).
- Selig, E.T. & Waters, J.M. 1994. *Track Geotechnology and Substructure Management*. Thomas Telford Ltd., London, England.
- Solomon, B. 2001. *Railway Maintenance Equipment: The Men and Machines that Keep the Railroads Running*. MBI Publishing Company LLC., Minneapolis, Minnesota, USA.
- Sussmann, T.R., Selig, E.T., & Hyslip, J.P. 2003. Railway Track Condition Indicators from Ground Penetrating Radar. *NDT & E International*. Vol. 36, Issue 3, April 2003, pp. 157-167.
- Thompson, H.B. & Carr, G. 2014. *Ground Penetrating Radar Evaluation and Implementation*. United States Department of Transportation (USDOT) Federal Railroad Administration (FRA), Research Results 14-24, July 2014.
- Wolf, H.E. 2015. *Flexural Behavior of Prestressed Concrete Monoblock Crossties*. M.S. Thesis 2015. University of Illinois at Urbana-Champaign, Urbana, Illinois, USA.
- Wolf, H.E., Qian, Y., Edwards, J.R., Dersch, M.S., & Lange, D.A. 2016. Temperature-induced curl behavior of prestressed concrete and its effect on railroad crossties. *Construction and Building Materials*. 115 (2016), 319-326.